J Mol Model (2019) 25: 20
https://doi.org/10.1007/s00894-018-3907-1

ORIGINAL PAPER

Understanding the nature of bonding interactions in the carbonic acid dimers

Andy D. Zapata–Escobar[1] · Juliana Andrea Murillo–López[2] · C. Z. Hadad[1] · Albeiro Restrepo[1]

Received: 2 May 2018 / Accepted: 13 December 2018 / Published online: 4 January 2019

Abstract

Carbonic acid dimer, $(CA)_2$, $(H_2CO_3)_2$, helps to explain the existence of this acid as a stable species, different to a simple sum between carbon dioxide and water. Five distinct, well characterized types of intermolecular interactions contribute to the stabilization of the dimers, namely, C=O···H–O, H–O···H–O, C=O···C=O, C=O···O–H, and C–O···O–H. In many cases, the stabilizing hydrogen bonds are of at least the same strength as in the water dimer. We dissect the nature of intermolecular interactions and assess their influence on stability. For a set of 40 $(H_2CO_3)_2$ isomers, C=O···H–O hydrogen bonds between the carbonyl oxygen in one CA molecule and the acidic hydrogen in the hydroxyl group at a second CA molecule are the major stabilizing factors because they exhibit the shortest interaction distances, the largest orbital interaction energies, and the largest accumulation of electron densities around the corresponding bond critical points. In most cases, these are closed-shell hydrogen bonds, however, in a few instances, some covalent character is induced. Bifurcated hydrogen bonds are a common occurrence in the dimers of carbonic acid, resulting in a complex picture with multiple orbital interactions of various strengths. Two *anti–anti* monomers interacting via the strongest C=O···H–O hydrogen bonds are the ingredients for the formation of the lowest energy dimers.

Keywords Carbonic acid · QTAIM · NBOs · Hydrogen bonds · Bifurcated bonds

Introduction

Carbonic acid, CA, H_2CO_3, is a relatively stable oxacid [1–7], postulated for a long time and first observed in 1987 during the decomposition of $(NH_4)HCO_3$ [1]. CA was first synthesized in 1991 [8]. CA is involved in a large number of fundamental processes, such as blood pH regulation [9–11], as an intermediate of CO_2 exhaustion during breathing [12, 13], and as a major player in oceanic CO_2 absorption, leading to the acidification of surface waters [14–16]. CA has been found in comets [17], interstellar space [18], planetary [19, 20] and lunar surfaces [21], and in our own atmosphere [2, 22, 23]. H_2CO_3 molecules exist in three conformational isomers because of the internal rotation of the O–H bonds in hydroxyl groups. At the QCISD(T)/6–311++G** level [24], in the lowest energy structure, hydrogen atoms adopt an *anti–anti* (**aa**) conformation, the *anti–syn* monomer (**as**) is located 1.9 kcal mol^{-1} above, and the *syn–syn* (**ss**) is 11.8 kcal mol^{-1} above **aa**. All CA monomers are depicted in Fig. 1.

A number of thermodynamically and kinetically controlled processes heavily dependent on the chemical environment affect the stability of CA molecules, among them, acid dissociation, dimerization, double proton transfer, and decomposition, are recognized as the most influential. Aqueous H_2CO_3 is unstable towards decomposition because upon dissolving CO_2 in H_2O, the few H_2CO_3 molecules formed immediately decompose in an exothermic reaction, due to the presence of surrounding water molecules [24, 25]. Furthermore, some theoretical works suggest that gas-phase carbonic acid easily decomposes into CO_2 and H_2O even in the absence of water [26–28]. Carbonic acid compensates its instability by forming molecular dimers [4], which appear to be the most abundant form of

Electronic supplementary material The online version of this article (https://doi.org/10.1007/s00894-018-3907-1) contains supplementary material, which is available to authorized users.

✉ Albeiro Restrepo
albeiro.restrepo@udea.edu.co

[1] Instituto de Química, Universidad de Antioquia UdeA, Calle 70 No. 52–21, Medellín, Antioquia, 050010, Colombia

[2] Departamento de Ciencias Químicas, Facultad de Ciencias Exactas, Universidad Andres Bello, República 275, Santiago, Chile

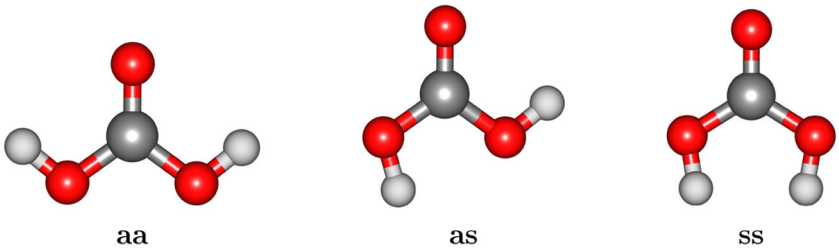

Fig. 1 Low energy conformations of H_2CO_3: *anti–anti*, *anti-syn*, and *syn–syn*

CA. Indeed, the experimental IR spectra of bulk H_2CO_3 resemble the simulated spectrum of the dimer rather than those of the monomers [25, 29]. In order to explain the high stability of carbonic acid dimers, several theoretical works have been carried out using different low-energy configurations of $(H_2CO_3)_2$ [4, 25, 29–34]. Also, there are several theoretical studies related to carbonic acid aggregates of higher molecularities [2, 25, 29–31, 35, 36], whose stability is mostly considered to come from cooperative networks of hydrogen bonds (HBs) [33, 34]. The physical origins of HBs are not without controversy, specifically, the classical view of dipolar interactions has been invoked to rationalize hydrogen bonds among a set of carbonic acid dimers [29], however, this approach conceals the quantum mechanical aspects of the interactions involved in chemical bonding.

In general terms, the stabilities, structures, and properties of atomic or molecular clusters largely depend on how the different units interact with each other. Thus, a detailed knowledge of the nature of stabilizing interactions is of pivotal importance. Accordingly, there are a number of computational chemistry-based methods that help in the quantum mechanical examination of intra and intermolecular interactions. Among the existing theoretical tools, we are especially interested in the quantum theory of atoms in molecules, (QTAIM) [37], and the natural bond orbitals (NBOs) analyses of bonding interactions [38–40]. QTAIM and NBO are appropriate models to characterize aggregates of atoms or molecules, using, respectively, the topology of electron densities and localized orbitals. They have been specially useful in finding and dissecting known as well as new forms of interactions in a wide variety of systems, including several kinds of pure and charged-assisted hydrogen bonds [41–49] and metallic clusters [50, 51], in following the evolution of chemical reactions [52–54], and as an effective tool to understand molecular structure and bonding [55–61].

Despite the interest and progress concerning hydrogen bonding, the dimers of carboxylic acids, and specifically the carbonic acid dimer, a quantum mechanical description of the nature of the stabilizing intermolecular interactions is insufficient. For this reason, in the current work, we delve at a fundamental level into the nature of the intermolecular contacts that keep the dimers of carbonic acid as stable discrete units.

Methods

The most comprehensive work to date dealing with the structural diversity of the dimers of carbonic acid was provided by Murillo and coworkers [32]. The authors considered all possible combinations of monomers to produce dimers. In this work, we analyze the bonding interactions in the 40 well-defined minima in the $(CA)_2$ MP2/6–311++G(d, p) potential energy surface (PES) located by Murillo et. al., and use the same nomenclature to address individual structures.

The quantum theory of atoms in molecules (QTAIM) [37], is one of the theoretical tools used here for the characterization of intermolecular interactions. QTAIM is based on topological analysis of the electron density of the system of interest. The points where the gradient of the electron density vanishes, $\vec{\nabla}\rho(\mathbf{r}_c) = 0$, define the critical points, CPs. Electron distributions may have different curvatures at CPs, thus, local extrema are categorized by means of the eigenvalues of the Hessian matrix of the electron density as nuclear (NCP), non-nuclear attractors (NNACP), bond (BCP), ring (RCP), and cage (CCP) critical points. The BCPs contain a wealth of information that when properly treated provide accurate descriptions of the interactions between two atoms; accordingly, we use the properties of these points to analyze the carbonic acid dimers. All the electron density properties reported in this contribution were obtained by means of the AIMALL package [62].

A number of QTAIM-based relationships were used to characterize all intermolecular interactions in the $(H_2CO_3)_2$ structures. They are defined in such a way as to facilitate the classification of the intermolecular interactions by their degree of covalency. Three central quantities to this purpose, evaluated at BCPs, are the Laplacian of the electron density, $\nabla^2\rho(\mathbf{r}_c)$, the ratio between the absolute value of potential energy density to the kinetic energy density, $|\mathscr{V}(\mathbf{r}_c)|/\mathscr{G}(\mathbf{r}_c)$ [63], and the ratio of the total energy density, $\mathscr{H}(\mathbf{r}_c) = \mathscr{V}(\mathbf{r}_c) + \mathscr{G}(\mathbf{r}_c)$, to the electron density, $\mathscr{H}(\mathbf{r}_c)/\rho(\mathbf{r}_c)$. If $\nabla^2\rho(\mathbf{r}_c) < 0$, $\mathbf{r}_c$ defines a local maximum and thus the electron density is concentrated in the internuclear region and the bond is covalent. If $\nabla^2\rho(\mathbf{r}_c) > 0$, $\mathbf{r}_c$ defines a local minimum of electron density and thus there is a depletion of charge around the BCP and a consequential

accumulation of electron density surrounding the two atoms connected by the bonding path, thus, these interactions are of closed-shell nature (for example, weak to intermediate strength forms of hydrogen bonds and van der Waals interactions). Interestingly, closed-shell interactions can still be cataloged, approximately, as interactions with a certain covalent character when $1 < |\mathscr{V}(\mathbf{r}_c)|/\mathscr{G}(\mathbf{r}_c) < 2$ and $\mathscr{H}(\mathbf{r}_c)/\rho(\mathbf{r}_c) < 0$ [59]. This is because the potential energy is always negative (attractive) and the kinetic energy is always positive (repulsive), thus, if $|\mathscr{V}(\mathbf{r}_c)|/\mathscr{G}(\mathbf{r}_c) > 1 \Longrightarrow |\mathscr{V}(\mathbf{r}_c)| > \mathscr{G}(\mathbf{r}_c)$, then, the excess of stabilizing potential energy at the bond critical point is an indication of some degree of concentration of electron density, resulting in a shared-like character for the interaction.

It is worth mentioning at this point that several alternative approaches to dissect the nature of interactions have recently emerged in the scientific literature within the QTAIM framework [64–69]. The main idea behind many of the new approaches is that local properties of the BCPs provide an incomplete picture of the energetics associated with the interactions and therefore other energy-based criteria and non-local properties are needed. See for example the work by Lane and coworkers [70] as one particular example where the very existence of bond critical points is questioned as needed for the characterization of hydrogen bonds. Accordingly, we computed the components of the atomic contributions to diatomic interaction energies via the interacting quantum atoms (IQAs) [71–73]. Specifically, we calculated diatomic interactions for those pairs of atoms linked by intermolecular BCPs, i.e., all O···H contacts in hydrogen bonds, and all the C···O, O···O pairs in the less common intermolecular interactions also found here.

A complementary manner to study interactions among atomic or molecular units is by means of orbital overlap. Especially useful for this purpose are the natural bond orbitals, NBOs [38–40], which are set of localized Lewis-like orbitals. NBOs are obtained as linear combinations of hybridized natural orbitals, each being an optimized linear combination of natural atomic orbitals, as described elsewhere [39, 40]. Because of their localized Lewis-like nature, NBOs provide a chemically intuitive and yet quantum mechanically rigorous description of intermolecular interactions in a molecular cluster. Generally speaking, the nature and strength of one particular interaction is described by the overlap between NBOs belonging to different units within the clusters, with one occupied NBO (ϕ_o) acting as donor and one virtual NBO (ϕ_v) as acceptor of electron charge, the stabilization energy, $E_{ov}^{(2)}$, afforded by the interaction is given to a second order in perturbation theory by

$$E_{ov}^{(2)} = -q_o \frac{|\langle \phi_o | \mathcal{F} | \phi_v \rangle|^2}{\varepsilon_o - \varepsilon_v} \quad (1)$$

where q_o is the occupancy of the donor orbital, ε_o and ε_v are the corresponding orbital energies, and $\mathcal{F}$ is the Fock operator. The wave functions needed for NBO computations were obtained using Gaussian 09 [74]. All NBO-related quantities were calculated using NBO6.0 [75].

Results and discussion

The first attempt to rationalize the nature of the interactions leading to stabilization in the studied extensive list of carbonic acid dimers was provided by Murillo and coworkers [32]. An intuitive, well-supported classical electrostatic picture emerged to explain the geometrical preferences of the hydrogen bond networks. It was qualitatively shown that the arrangements of dipole moments in polar bonds produced the most favorable electrostatic configurations in the 40 reported molecular geometries. However, rigorous calculations of interaction energies using this model were not possible because the authors pointed out that the multipole expansion approximation [76] requires ideal dipoles and dipole↔dipole separations very large compared to the sizes of individual dipoles, conditions that are clearly not met in molecular clusters. In lieu of actual electrostatic stabilization energies using the multipole expansion, the authors showed a good correlation between the total electrostatic energy calculated for all point charges at the positions of the atoms belonging to dipole components along the hydrogen bond network, and binding energies.

Topological analysis of electron densities

The structures and corresponding QTAIM-based intermolecular connections for the dimers of carbonic acid are depicted in Fig. 2. The wide spectrum of structural possibilities is due to five types of well-characterized stabilizing intermolecular contacts dictated by bonding paths, summarized as follows: (*i*) hydroxyl to carbonyl C=O···H–O hydrogen bonds (all HBs in structure 1, Fig. 2, for example) (*ii*) hydroxyl to hydroxyl H–O···H–O hydrogen bonds (top hydrogen bond in structure 4, Fig. 2, for example) (*iii*) carbon to carbonyl C=O···C=O contacts (interaction at the bottom of structure 10, Fig. 2, for example) (*iv*) carbonyl to hydroxyl C=O···O–H contacts (O···O interaction in structure 34, Fig. 2, for example) (*v*) hydroxyl to hydroxyl H–O···O–H contacts (O···O interaction in structure 35, Fig. 2, for example).

As inferred from Table 1, hydroxyl to carbonyl C=O···H–O hydrogen bonds are the strongest intermolecular interactions in the carbonic acid dimers. In fact, they are the only ones that could be characterized as being of intermediate character with contributions from both closed-shell and covalent interactions according to the $|\mathcal{V}(\mathbf{r}_c)|/\mathcal{G}(\mathbf{r}_c)$

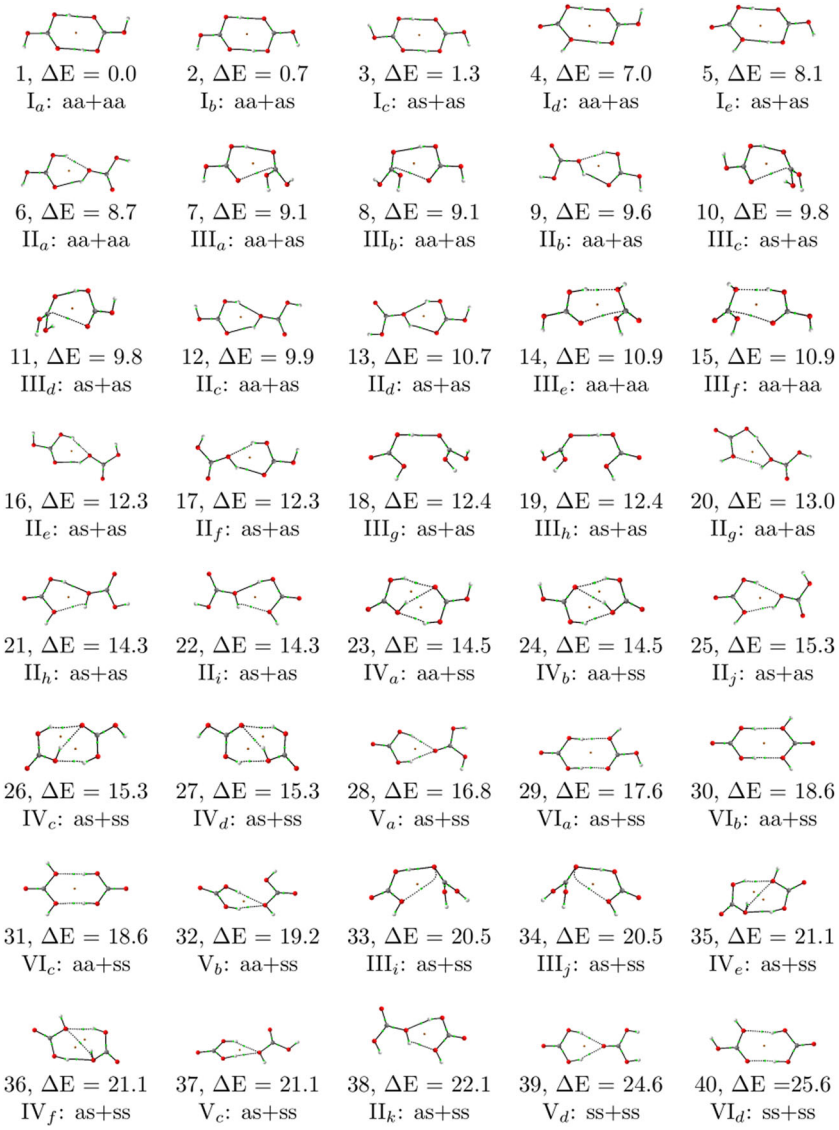

Fig. 2 Molecular structures for the 40 isomers of $(H_2CO_3)_2$. QTAIM derived bond paths are shown. Relative energies, ΔE, are reported in kcal mol^{-1} at the CCSD(T)/aug-cc-pvdz level, calculated on the MP2/6–311++G(d, p) optimized geometries. Structures and energies as reported in the work of Murillo and coworkers [32]

criterion suggested by Espinosa and coworkers [63] as discussed in the Introduction. Interestingly, according to QTAIM criteria, this type of hydrogen bond is in many instances stronger than HBs in the water dimer. Furthermore, C=O···H–O interactions are the only ones that show cases of negative values for $\mathscr{H}(\mathbf{r}_c)$ (structures 1, 2, 3, 4, and 5 in Fig. 3), thus reflecting the accumulation of electron density at the critical point, and revealing some degree of covalency, despite the Laplacian of the electron density being larger than zero (local minimum in electron density).

Table 1 Limits for the minimum and maximum values for geometrical (Å) and QTAIM (a.u.) derived quantities at intermolecular bond critical points for the 40 dimers of carbonic acid in Fig. 2

Interaction type	**r**	$\rho(\mathbf{r}_c)\times10^3$	$\nabla^2\rho(\mathbf{r}_c)\times10^3$	$\mathscr{H}(\mathbf{r}_c)\times10^3$	$\lvert\mathscr{V}(\mathbf{r}_c)\rvert/\mathscr{G}(\mathbf{r}_c)$
C=O···H–O	1.65, 2.12	20.63, 48.03	72.02, 146.29	-6.12, 2.70	0.87, 1.14
H–O···H–O	1.80, 2.20	15.51, 32.90	63.55, 120.73	0.25 , 2.59	0.84, 0.99
O···C	2.81, 2.96	8.51, 11.89	35.25, 44.99	1.17, 1.25	0.83, 0.88
O···O	2.87, 3.02	8.48, 12.84	36.22, 48.89	1.10, 1.40	0.82, 0.90
H_2O···H–O–H	1.98	23.20	91.51	2.34	0.89

Analogous quantities for the water dimer are included for comparison

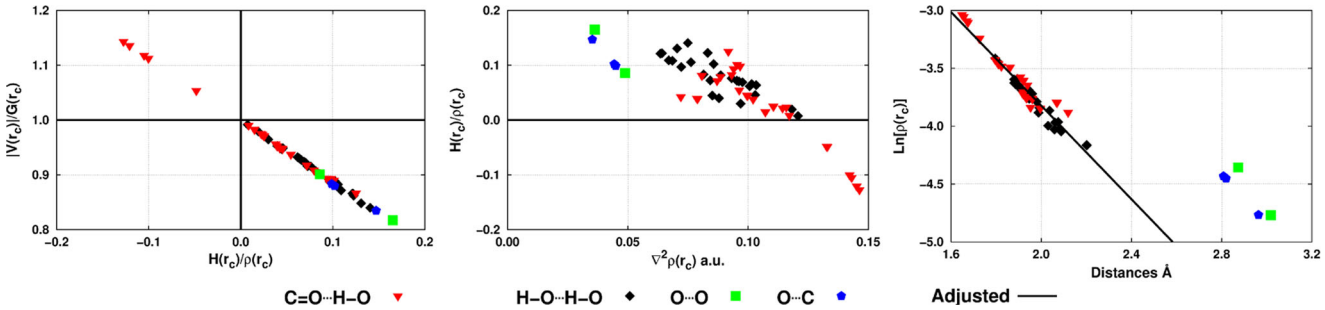

Fig. 3 QTAIM-derived quantities at bond critical points for the intermolecular interactions shown in Fig. 2. *Left*: Ratio of the absolute value of potential energy density to kinetic energy density against the bond parameter $\mathcal{H}(\mathbf{r}_c)/\rho(\mathbf{r}_c)$ [63]. *Center*: Total energy density against the Laplacian of the electron density. *Right*: Exponential decay of the electron density as a function of the interaction distance. The R^2 value of the adjusted line is 0.94

Hydroxyl to hydroxyl H–O···H–O hydrogen bonds also have QTAIM derived properties at bond critical points that characterize them as being of at least the same strength of hydrogen bonds in the water dimer (Table 1). Our results show that because C=O···H–O and H–O···H–O are the most frequent and the strongest intermolecular contacts, they are the primary factors that stabilize the carbonic acid dimers.

We argue that C=O···H–O and H–O···H–O interactions are closely related at a fundamental level because calculated properties at their bond critical points are tightly packed around the closed-shell/intermediate character boundary ($|\mathcal{V}(\mathbf{r}_c)|/\mathcal{G}(\mathbf{r}_c) \approx 1$) and around the covalent/non–covalent ($\mathcal{H}(\mathbf{r}_c)/\rho(\mathbf{r}_c) \approx 0$) boundary in the left panel of Fig. 3. Further analysis, beyond the scope of this work, is lacking in the scientific literature discussing the meaning of properties obtained at the vicinities of the rigid boundaries of QTAIM-derived criteria, for cases such as those obtained here. Nonetheless, a number of useful observations may be drawn from this plot: (*i*) C=O···H–O interactions appear to be the strongest, as indicated by larger $|\mathcal{V}(\mathbf{r}_c)|/\mathcal{G}(\mathbf{r}_c)$ and by more negative $\mathcal{H}(\mathbf{r}_c)/\rho(\mathbf{r}_c)$ values (*ii*) there is a region of overlap between the C=O···H–O and H–O···H–O interactions, however, it is clear that only a number of C=O···H–O contacts have negative $\mathcal{H}(\mathbf{r}_c)/\rho(\mathbf{r}_c)$ (which simultaneously have the largest $|\mathcal{V}(\mathbf{r}_c)|/\mathcal{G}(\mathbf{r}_c)$) and that a few of the H–O···H–O interactions clearly have the smallest ratios of potential to kinetic energy densities while simultaneously having positive total energy densities (*iii*) the exotic C···O and O···O interactions fall in the same range as the weakest hydroxyl to hydroxyl hydrogen bonds. As mentioned above, some C=O···H–O interactions have negative values for $\mathscr{H}(\mathbf{r}_c)$, thus reflecting the dominance of the stabilizing potential energy term, which in turns leads to accumulation of electron density at the critical point, revealing some degree of covalency, despite the Laplacian of the electron density being larger than zero (center plot in Fig. 3). It has been shown elsewhere [46, 48, 59] that for hydrogen bonds with $\mathscr{H}(\mathbf{r}_c) < 0$, the covalent character confers additional stabilization to the interaction.

Very useful insight into the nature of bonding interactions can be obtained from the exponential decay of the electron densities at bond critical points as a function of bond distance shown in the right panel of Fig. 3. Armed with convincing evidence obtained by themselves and by other groups, Knop and coworkers [60] postulated that the electron densities at bond critical points (or better yet, functions of the electron densities) correlate with bond distances for any kind of binary bonds, no matter both the strength of the interactions and the identity of the involved molecular orbitals. Later, Alkorta and coworkers [61], in a study considering many types of bonds, determined exponential decays of the electron densities, a trend reproduced by Knop and coworkers for a large set of N–H···N hydrogen bonds [77, 78] and by others in several hydrogen bonding scenarios [41, 44]; nicely, the same behavior is equally reproduced here with outstanding agreement for the particular case of intermolecular interactions in the dimers of carbonic acid. The exponential decay is physically accurate because as separation distances increase beyond the point of interaction, electron densities at bond critical points vanish rather than becoming negative as linear trends may suggest. Equally important as the right asymptotic behavior is the fact that the two types of hydrogen bonds, acting as main stabilizing factors in the dimers of carbonic acid (C=O···H–O and H–O···H–O), obey the same exponential decay, thus, they have the same physical origins and can be told apart from other types of interactions that obey other rules, in particular, as evident from Fig. 3, non-traditional O···O and C···O intermolecular contacts seem to obey quite different trends. Finally, we point out that as suggested by Bader and Essen [79], C=O···H–O and H–O···H–O interactions can be truly characterized as hydrogen bonds

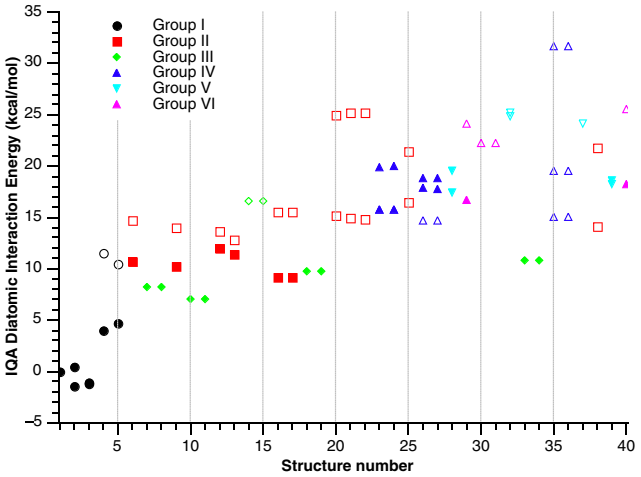

Fig. 4 Relative IQA diatomic interaction energies for all hydrogen bonds in the structures shown in Fig. 2 according to the groups of geometrical motifs defined by Murillo and coworkers [32]. Structure 1 was taken as a reference. *Filled symbols* correspond to C=O···H–O interactions and *unfilled symbols* denote C–O···H–O contacts. Notice that every point represents a particular interaction, thus, there are for example three points associated to structure 26, which has three HBs

because the electron densities at the corresponding critical points lead to positive Laplacians and are smaller than 0.1 a.u. (Table 1).

Diatomic interaction energies for the interacting quantum atoms for all hydrogen bonds in the structures shown in Fig. 2 are plotted in Fig. 4 according to the groups of geometrical motifs defined by Murillo and coworkers [32], the corresponding energy decomposition components are plotted in Fig. 5. Nicely, as a general rule, the same trend as in stabilization energies is obtained, namely, relative IQAs for group I appear below IQAs for group II in Fig. 4, and so on.

A closer look at Figs. 4 and 5 reveals the following interesting points:

1. As discussed above, and in qualitative agreement with the results listed in Table 1, IQA interaction energies characterize C=O···H–O hydrogen bonds as more stabilizing than C–O···H–O. As a particular example, there is ≈ 6.6 kcal/mol difference in IQA interaction energies between C=O···H–O and C–O···H–O for structures 4 and 5.
2. Not all C=O···H–O interactions are the same. As a particular example, there is ≈ 5.5 kcal/mol IQA interaction energy difference between the same intermolecular contact in structures 2 and 4. This difference is easily rationalized because (V_{ne}), the attractive nuclei–electrons energy, favors structure 2 (Fig. 5).
3. IQA interaction energies show that there is added stabilizing power in cumulative bifurcation. Compare for example in Fig. 4 structure 28 (group V, two bifurcated hydroxyl to carbonyl HBs) against structure 29 (group VI, one hydroxyl to carbonyl and one hydroxyl to hydroxyl HB).
4. The exotic O···C intermolecular contacts are stabilizing while O···O are destabilizing. This statement is backed up by Table 2, listing IQA interaction energies along with the corresponding decomposition.

It is very interesting to notice that C···O IQA interaction energies are even more stabilizing than the most stabilizing hydrogen bond! This explains why they appear as early as in structures 7 and 8 in Fig. 2. This unexpectedly large stabilization is understood as a consequence of the balance between the repulsive nuclear–nuclear V_{nn}, and Coulomb electronic V_{ee}^{C} terms, which have a combined smaller magnitude than the combined stabilizing V_{ne}, V_{en}

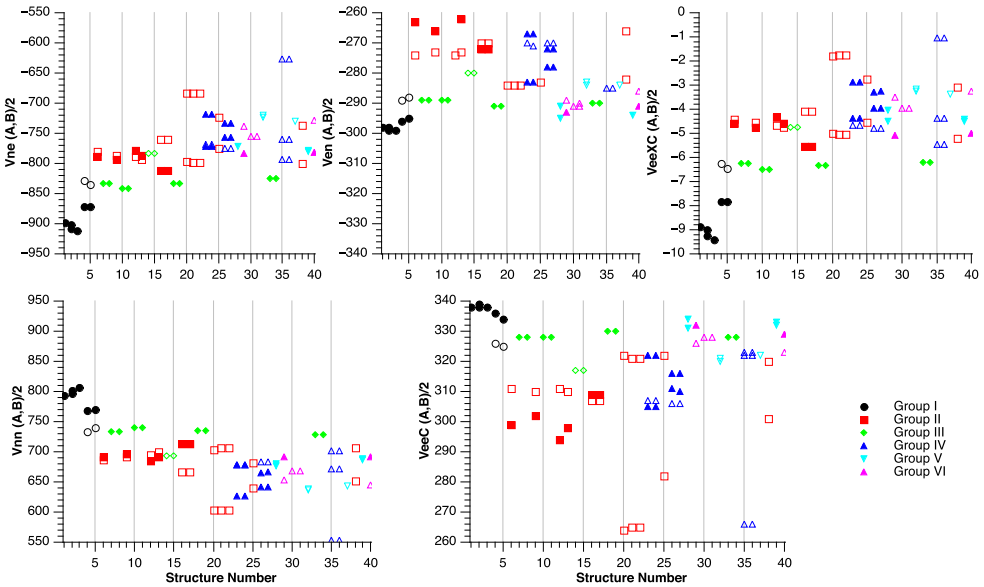

Fig. 5 IQA atomic contributions to the diatomic interaction energy components for each structure in Fig. 2. The meaning of each term was defined elsewhere [71, 72]. *Filled symbols* correspond to C=O···H–O interactions and *unfilled symbols* denote C–O···H–O contacts

Table 2 IQA contribution to average diatomic interaction energy components for C···O and O···O interactions (atomic units)

Interaction type	V_{ne}(A,B)/2	V_{en}(A,B)/2	V_{nn}(A,B)/2	V_{ee}^{C}(A,B)/2	V_{ee}^{XC}(A,B)/2	E_{IQA}^{inter}(A,B)/2
H···O	-1.4331	-0.4756	1.2636	0.5392	-0.0141	-0.1200
C···O	-5.0734	-2.8745	4.4376	3.2860	-0.0021	-0.2264
O···O	-6.4928	-6.4828	5.7175	7.3618	-0.0035	0.1002

The most stabilizing HB interaction in Structure 1 (Fig. 2) was taken as reference. See definition of terms in [71, 72]

terms. The opposite effect, that is, larger combined repulsive terms, is revealed for the O···O case.

Natural bond orbital analysis

We study the intermolecular interactions from the perspective of the contributions to stabilization from charge transfer among molecular orbitals within the NBO frame. In addition, we analyze in detail the orbital interactions leading to bifurcated hydrogen bonds.

Within NBO, hydrogen bonds arise from electron delocalization in the form of charge transfer between localized occupied and virtual molecular orbitals in the involved molecular units [80]. For the archetypal hydrogen bond in the water dimer, a non-bonding lone pair in one of the oxygen atoms transfers charge to an antibonding orbital in the second molecule $\left(n_O \rightarrow \sigma^*_{OH}\right)$ [81]. In this work, we found that hydrogen bonds in the dimers of carbonic acid seem to obey the same basic charge transfer rule in a considerably more complex scenario, with multitude of orbital pairs involved. For C=O···H–O and H–O···H–O, the two major contributors to CA_2 stabilization, all involved orbital interactions are listed in Table 3, along with the corresponding interaction energies.

Table 3 NBO contributions to the C=O···H–O and H–O···H–O hydrogen bonds in the set of 40 carbonic acid dimers in Fig. 2

Interaction	Charge transfer	range for $E_{ov}^{(2)}$
		from Eq. 1
C=O···H–O	$n_O \rightarrow \sigma^*_{O\text{-}H}$	0.08 – 22.41
	$\pi_{C=O} \rightarrow \sigma^*_{O\text{-}H}$	0.05 – 3.34
	$\sigma_{O\text{-}H} \rightarrow \pi^*_{C=O}$	0.05 – 0.37
H–O···H–O	$n_O \rightarrow \sigma^*_{O\text{-}H}$	0.05 – 11.55
	$\sigma_{O\text{-}H} \rightarrow \sigma^*_{O\text{-}H}$	0.05 – 0.25
H_2O···H–O–H	$n_O \rightarrow \sigma^*_{O\text{-}H}$	≈ 5.4 [81]

The corresponding entries reported by Reed and Weinhold [81] for an idealized water dimer are included for comparison. Interaction energies in kcal/mol

Noticeably, for a single hydrogen bond, multiple charge transfer interactions with significant energies between orbital pairs are possible. Despite QTAIM and NBO resting on very different theoretical grounds, a remarkable agreement between the two descriptions of stabilizing interactions in the carbonic acid dimers is obtained. Especially meaningful is the realization by both methodologies that hydrogen bonds are considerably stronger in several CA_2 cases than in the water dimer, as indicated by larger electron densities and larger $|\mathcal{V}|/\mathcal{G}$ ratios at bond critical points (Table 1) and by larger orbital interaction energies (Table 3).

Bifurcated hydrogen bonds

Bifurcated hydrogen bonds are well known and come in two structural varieties; on one hand, those where one single hypercoordinate hydrogen atom acts as donor to two different hydrogen bonds are known as "bifurcated donors"; on the other hand, those cases where a single electronegative atom acts as acceptor of two hydrogen bonds are termed "bifurcated acceptors". The two available lone pairs of individual oxygen atoms contained in a variety of functional groups render bifurcated acceptors a common occurrence. Notice that since the two lone pairs on the same atom are not equivalent, individual interactions with other orbitals may have different energies. Figure 2 indicates that among the carbonic acid dimers, structures 23, 24, 26, 27, 28, 32, 37, and 39, belong to the bifurcated acceptor type. There is a significant amount of literature reporting experimental [82] and theoretical [83] studies of bifurcated hydrogen bonds, for a comprehensive review on the subject, see for example the treatise by the Gillies [84]. We offer here an analysis of the orbital interactions leading to bifurcated hydrogen bonds.

Symmetric bifurcated acceptor hydrogen bonds

Structures 28, 32, 37, and 39 in Fig. 2 exhibit two apparently equivalent bifurcated hydrogen bonds, thus, we assign them to the "symmetric" category. Two subcategories arise here, those where the bifurcated acceptor is an oxygen atom in a carbonyl group (structures 28 and 39) and those where the

bifurcated acceptor is an oxygen atom in a hydroxyl group (structures 32 and 37).

For the bifurcated oxygens in C=O, there are two different lone pairs to donate charge and two different receptor antibonding orbitals, thus, four distinct $n_O \rightarrow \sigma^*_{OH}$ are detected. For structure 39, those seem to be the major stabilizing factors, with $E^{(2)}_{ov} = 3.78, 3.67$ kcal/mol from one n_O orbital to each of the two neighboring antibonding orbitals and 2.75, 2.48 kcal/mol from the other lone pair to each of the same σ^*_{OH} orbitals. Smaller stabilization energies arise from $\pi_{C=O} \rightarrow \sigma^*_{O\text{-}H}$ (0.36, 0.34 kcal/mol) and from $\sigma_{O\text{-}H} \rightarrow \pi^*_{C=O}$ (0.22, 0.22 kcal/mol). The two bifurcated hydrogen bonds in structure 39 have $\rho = 0.023, 0.024$, and $|\mathcal{V}|/\mathcal{G} = 0.89, 0.89$ at the critical points; thus they are at least of comparable strength as hydrogen bonds in the water dimer (Tables 1 and 3).

For the bifurcated hydrogens in hydroxyl groups, only the charge transfer contributions from the lone pairs of the oxygen atom in the O–H bond in one molecule to the neighboring antibonding orbitals in the second molecule are significant. Thus a total of four distinct $n_O \rightarrow \sigma^*_{OH}$ are detected. For structure 37, the corresponding interactions energies are $E^{(2)}_{ov} = 2.90, 2.91$ kcal/mol from one n_O orbital to each of the two neighboring antibonding orbitals and 1.14, 1.14 kcal/mol from the other lone pair to the same σ^*_{OH} orbitals. The two bifurcated hydrogen bonds in structure 37 have $\rho = 0.019, 0.019$, and $|\mathcal{V}|/\mathcal{G} = 0.89, 0.89$ at the critical points. Thus, as in the symmetric bifurcated oxygen atoms in the carbonyl group, these hydrogen bonds are at least of comparable strength (perhaps just a little weaker because of the orbital interaction energies) as hydrogen bonds in the water dimer (Tables 1 and 3).

Non-symmetric bifurcated acceptor hydrogen bonds

Structures 23, 24, 26, and 27 in Fig. 2 exhibit two apparently non-equivalent bifurcated hydrogen bonds. Thus, we assign them to the "non-symmetric" category. In all cases, an acceptor oxygen from a carbonyl group is involved. The orbital interaction picture is a bit more complex here than in the symmetric case. The breaking of symmetry is caused by the fact that some of the a priori equivalent interactions lead to different energies. Take for example structure 23, there, as opposed to the symmetric case, interactions energies are $E^{(2)}_{ov} = 3.06, 0.48$ kcal/mol from one n_O orbital to each of the two neighboring antibonding orbitals and 2.76, 2.37 kcal/mol from the other lone pair to each of the same σ^*_{OH} orbitals. Smaller contributions also arise from other interactions. On the basis of NBO interactions energies (Table 3), and electron densities and potential to kinetic energy ratios at bond critical points (Table 1), at least one of the non-symmetric bifurcated hydrogen bonds should be of about the same strength as the hydrogen bond in the water dimer.

Conclusions

We summarize the most important findings of our work as follows:

1. Five well-characterized types of intermolecular interactions stabilize the dimers: conventional C=O···H–O and H–O···H–O hydrogen bonds, as well as less common C=O···C=O, C=O···O–H, and C–O···O–C contacts.
2. Largest orbital interaction energies, largest accumulation of electron densities around the corresponding bond critical points, and other QTAIM-derived criteria suggest that C=O···H–O hydrogen bonds are the strongest stabilizing factors, followed by H–O···H–O HBs.
3. In many cases, the stabilizing interactions are stronger, or at least of the same magnitude, as in the archetypal hydrogen bond in the water dimer.
4. Bifurcated hydrogen bonds are common in the dimers of carbonic acid, we divide them into two structural categories: symmetric and non-symmetric. In the symmetric cases, both HBs are at least as strong as in the water dimer case. In the non-symmetric cases, despite being of the same structural type, one of the hydrogen bonds is strong and the other is weak.
5. Most intermolecular contacts are characterized as long-distance, closed-shell hydrogen bonds. However, in some unusually strong C=O···H–O instances, some degree of covalency is observed.
6. Contrary to the water dimer and other simple cases, hydrogen bonds in the carbonic acid dimers arise from multiple contributions in the form of charge transfer between several pairs of molecular orbitals.
7. The IQA results are in line with the conclusions drawn from QTAIM and NBO, characterizing C=O···H–O hydrogen bonds as more stabilizing than C–O···H–O. Additionally, IQA suggest that C···O contacts are stabilizing while O···O are destabilizing. Interestingly, IQA suggests that C···O interaction energies are even more stabilizing than the most stabilizing hydrogen bond.

Acknowledgements Financial support for this project by Colciencias via project 111571249844, contract 378–2016 is acknowledged. J.M. acknowledges CONICYT for her postdoctoral Project FONDECYT/Postdoctorado-2015 No. 3150041.

Funding Information Colciencias, Colombia: Project 111571249844, contract 378–2016. Conicyt, Chile: Fondecyt project, Postdoctorado–2015 No. 3150041.

Supporting Information Cartesian coordinates for all dimers considered in this work. QTAIM quantities evaluated at all bond critical points.

Abbreviations QTAIM:, Quantum theory of atoms in molecules.; BCPs:, Bond critical points.; NBOs:, Natural bond orbitals.

References

1. Terlouw J, Lebrilla C, Schwarz H (1987) Angew Chem Int Ed Engl 26:354
2. Hage W, Liedl K, Hallbrucker A (1998) E Mayer Sci 279:1332
3. Hage W, Hallbrucker A, Mayer E (1993) J Am Chem Soc 115:8427
4. Liedl K, Sekušak S, Mayer E (1997) J Am Chem Soc 119:3782
5. Loerting T, Tautermann CS, Kroemer R, Kohl I, Hallbrucker A, Mayer E, Liedl K (2000) Angew Chem Int Ed Engl 39:891
6. Al-Hosney H, Grassian V (2004) J Am Chem Soc 126:8068
7. Al-Hosney H, Grassian V (2005) Phys Chem Chem Phys 7:1266
8. Moore M, Khanna R (1991) Spectrochim Acta Part A 47A:255
9. Breg J, Tymoczko J, Stryer L, Biochemistry WH (2002) 5th edn. Freeman and company, New York
10. Lindskog S, Coleman JE (1973) Proc Natl Acad Sci USA 70:2505
11. Kern DM (1960) J Chem Educ 37:14
12. Fisher S, Maupin C, Budayova–Spano M, Govindasamy L, Tu C, Agbandje-Mckenna M, Silverman D, Voth G, McKenna R (2007) Biochemistry 46:2930
13. Thoms S (2002) J Theor Biol 215:399
14. Sabine CL, Feely RA, Gruber N, Key RM, Lee K, Bullister JL, Wanninkhof R, Wong CS, Wallace DWR, Tilbrook B, Millero FJ, Peng T, Kozyr A, Ono T, Rios AF (2004) Science 305:367
15. Orr JC, Fabry VJ, Aumont O, Bopp L, Doney SC, Feely RA, Gnanadesikan A, Gruber N, Ishida A, Joos F, Key RM, Lindsay K, Maier-Reimer E, Matear R, Monfray P, Mouchet A, Najjar RG, Plattner GK, Rodgers KB, Sabine CL, Sarmiento JL, Schlitzer R, Slater RD, Totterdell IJ, Weirig MF, Yamanaka Y, Yool A (2005) Nature 437:681
16. Dore J, Lukas R, Sadler W, Church M, Karl D (2235) Proc Natl Acad Sci USA 106(1):2009
17. Kim S, Minh Y, Hyung S, Kim Y, van Dishoeck E, van der Tak F (2000) High-Resolution Optical and Infrared Observations of Molecules in Comets: Chemistry in the Envelopes around Massive Young Stars from Molecular Clouds to Planetary, pp 471
18. Ehrenfreund PW, Schutte W (2000) Infrared Observations of Interstellar Ices, from Molecular Clouds to Planetary, pp 135
19. Longhi J (2006) J Geophys Res 111:E06011
20. Strazzulla G, Brucato JR, Cimino G, Palumbo ME (1996) Planet Space Sci 44:1447
21. Mason N et al (2006) VUV Spectroscopy of extraterrestrial ices, Astrochemistry-from Laboratory Studies to Astronomical Observations, pp 128
22. Ghoshal S, Hazra MK (2015) RSC Adv 5:17623
23. Chebbi A, Carlier P (1996) Atmos Environ 30:4233
24. Wight C, Boldyrev A (2125) J Phys Chem 99(1):1995
25. Tossell J (2006) Inorg Chem 45:5961
26. de Marothy SA (2013) Int J Quantum Chem 113:2306
27. Ghoshal S, Hazra MK (2014) J Phys Chem A 118:2385
28. Kumar M, Busch DH, Subramaniam B, Thompson WH (2014) J Phys Chem A 118:5020
29. Mitterdorfer C, Bernard J, Klauser F, Winkel K, Kohl I, Liedl K, Grothe H, Mayer E, Loerting T (2012) J Raman Spectrosc 43:108
30. Winkel K, Hage W, Loerting T, Price S, Mayer E (2007) J Am Chem Soc 129:13863
31. Ballone P, Montanari B, Jones R (2000) J Chem Phys 112:6571
32. Murillo J, David J, Restrepo A (2010) Phys Chem Chem Phys 12:10963
33. Ghoshal S, Hazra MK (2014) J Phys Chem A 118:4620
34. Tautermann CS, Voegele AF, Liedl K (2004) J Chem Phys 120:631
35. Nguyen M, Matus M, Jackson V, Ngan V, Rustad J, Dixon D (2008) J Phys Chem A 112:10386
36. Tossell J (2009) Environ Sci Technol 43:2575
37. Bader R (1990) Atoms in molecules. a quantum theory. Oxford University Press, NY
38. Weinhold F, Landis CR (2012) Discovering Chemistry wit Natural Bond Orbitals. Wiley
39. Reed A, Curtiss L, Weinhold F (1988) Chem Rev 88(6):89
40. Reed A, Weinhold F (1983) J Chem Phys 78:4066
41. Farfán P, Echeverri A, Diaz E, Tapia J, Gómez S, Restrepo A (2017) J Chem Phys 147:044312
42. Salazar J, Guevara A, Vargas R, Restrepo A, Garza J (2016) Phys Chem Chem Phys 18:23508
43. Pérez J, Hadad C, Restrepo A (2008) Intl J Quantum Chem 108:1653
44. Ramírez F, Hadad C, Guerra D, David J, Restrepo A (2011) Chem Phys Lett 507:229
45. Hincapié G, Acelas N, Castano M, David J, Restrepo A (2010) J Phys Chem A 114:7809
46. Acelas N, Hincapié G, Guerra D, David J, Restrepo A (2013) J Chem Phys 139:044310
47. Jenkins S, Restrepo A, David J, Yin D, Kirk SR (1644) Phys Chem Chem Phys 13(1):2011
48. Hadad C, Restrepo A, Jenkins S, Ramírez F, David J (2013) Theor Chem Acc 132:1376
49. Hadad C, Florez E, Acelas N, Merino G, Restrepo A (2018) Int J Quantum Chem 119(2). https://doi.org/10.1002/qua.25766
50. Yepes D, Kirk SR, Jenkins S, Restrepo A (2012) J Mol Model 18:4171
51. David J, Guerra D, Restrepo A (2012) Chem Phys Lett 64:539–540
52. Giraldo C, Gómez S, Weinhold F, Restrepo A (2016) Chem Phys Chem 17:2022
53. Gomez S, Guerra D, López JG, Toro–Labbé A, Restrepo A (2013) J Phys Chem A 117:1991
54. Mutlay I, Restrepo A (2015) Phys Chem Chem Phys 17:7972
55. Rengifo E, Gómez S, Arce J, Weinhold F, Restrepo A (2018) Comp Theor Chem 1130:58
56. Reed A, Weinhold F (1983) J Chem Phys 78:4066
57. Reed A, Curtiss L, Weinhold F (1998) Chem Rev 88:899
58. Weinhold F, Klein R (2014) Angew Chem Intl Ed 53:11214
59. Grabowski SJ (2011) J Chem Rev 111:2597
60. Knop O, Boyd R, Choi S (1998) J Am Chem Soc 110:7299
61. Alkorta I, Rozas I, Elguero J (1998) Struct Chem 9:243
62. Keith T (2013) AIMALL version 13.05.06. http://aim.tkgristmill.com/
63. Espinosa E, Alkorta I, Elguero J, Mollins E (2002) J Chem Phys 117:5529
64. Romero–Montalvo E, Guevara–Vela J, Vallejo W, Costales A, Martin A, Rodríguez M, Rocha–Rinza T (2017) Chem Comm 53:3516
65. Guevara–Vela J, Romero–Montalvo E, del Rio–Lima A, Martin A, Hernández–Rodríguez M, Rocha–Rinza T (2017) Chem Eur J 21:16605

66. Duarte V, Rocha–Rinza T, Cuevas G (2015) J Comp Chem 36:361
67. Guevara–Vela J, Romero–Montalvo E, Mora V, Chávez–Calvillo R, García–Revilla M, Francisco E, Martin A, Rocha–Rinza T (2016) Phys Chem Chem Phys 18:19557
68. Guevara–Vela J, Romero–Montalvo E, Costales A, Martin A, Rocha–Rinza T (2016) Phys Chem Chem Phys 18:26383
69. Guevara–Vela J, Chávez–Calvillo R, García–Revilla M, Hernández–Trujillo J, Christiansen O, Francisco E, Martin A, Rocha–Rinza T (2013) Chem Eur J 19:14304
70. Lane J, Contreras–García J, Piquemal J, Miller B, Kjaergaard H (2013) J Chem Theor Comp 9:3263
71. Blanco M, Pendás A, Francisco E (2005) J Chem Theory Comput 1:1096
72. Pendás A, Francisco E, Blanco M, Gatti C (2007) Chem Eur J 13:9362
73. Eskandari K, Val Alsenoy CJ (2014) Comp Chem 35:1883
74. Frisch MJ, Trucks GW, Schlegel HB, Scuseria GE, Robb MA, Cheeseman JR, Scalmani G, Barone V, Mennucci B, Petersson GA, Nakatsuji H, Caricato M, Li X, Hratchian HP, Izmaylov AF, Bloino J, Zheng G, Sonnenberg JL, Hada M, Ehara M, Toyota K, Fukuda R, Hasegawa J, Ishida M, Nakajima T, Honda Y, Kitao O, Nakai H, Vreven T, Montgomery Jr JA, Peralta JE, Ogliaro F, Bearpark M, Heyd JJ, Brothers E, Kudin KN, Staroverov VN, Keith T, Kobayashi R, Normand J, Raghavachari K, Rendell A, Burant JC, Iyengar SS, Tomasi J, Cossi M, Rega N, Millam JM, Klene M, Knox JE, Cross JB, Bakken V, Adamo C, Jaramillo J, Gomperts R, Stratmann RE, Yazyev O, Austin AJ, Cammi R, Pomelli C, Ochterski JW, Martin RL, Morokuma K, Zakrzewski VG, Voth GA, Salvador P, Dannenberg JJ, Dapprich S, Daniels AD, Farkas O, Foresman JB, Ortiz JV, Cioslowski J, Fox Dj (2013) Gaussian 09, Revision D.01, Gaussian, Inc., Wallingford CT
75. NBO 6.0, Glendening ED, Badenhoop JK, Reed A, Carpenter JE, Bohmann JA, Morales CM, Landis CR, Weinhold F (2013) Theoretical Chemistry Institute. University of Wisconsin, Madison. http://nbo6.chem.wisc.edu/
76. Jackson J (1998) Electrodynamics, 3rd edn. Classical Wiley, New York
77. Knop O, Rankin K, Boyd R (2001) J Phys Chem A 105:6552
78. Knop O, Rankin K, Boyd R (2003) J Phys Chem A 107:272
79. Bader R, Essen H (1984) J Chem Phys 80:1943
80. Reed A, Curtiss L, Weinhold F (1988) Chem Rev 88:899
81. Reed A, Weinhold F (1983) J Chem Phys 78:4066
82. Feldblum E, Arkin I (2014) Proc Natl Acad Sci 111:4085
83. Rozas I, Alkorta I, Elguero J (1998) J Phys Chem A 102:9925
84. Gilli G, Gilli P (2009) The nature of the hydrogen bond. Oxford University Press, New York